

Antarctic Circumpolar Current Transport Variability during 2003–05 from GRACE

VICTOR ZLOTNICKI

Jet Propulsion Laboratory, California Institute of Technology, Pasadena, California

JOHN WAHR

Cooperative Institute for Research in Environmental Sciences, and Department of Physics, University of Colorado, Boulder, Colorado

ICHIRO FUKUMORI AND YUHE T. SONG

Jet Propulsion Laboratory, California Institute of Technology, Pasadena, California

(Manuscript received 6 June 2005, in final form 6 June 2006)

ABSTRACT

Gravity Recovery and Climate Experiment (GRACE) gravity data spanning January 2003–November 2005 are used as proxies for ocean bottom pressure (BP) averaged over 1 month, spherical Gaussian caps 500 km in radius, and along paths bracketing the Antarctic Circumpolar Current's various fronts. The GRACE BP signals are compared with those derived from the Estimating the Circulation and Climate of the Ocean (ECCO) ocean modeling–assimilation system, and to a non-Boussinesq version of the Regional Ocean Model System (ROMS). The discrepancy found between GRACE and the models is $1.7 \text{ cm}_{\text{H}_2\text{O}}$ ($1 \text{ cm}_{\text{H}_2\text{O}} \sim 1 \text{ hPa}$), slightly lower than the $1.9 \text{ cm}_{\text{H}_2\text{O}}$ estimated by the authors independently from propagation of GRACE errors. The northern signals are weak and uncorrelated among basins. The southern signals are strong, with a common seasonality. The seasonal cycle GRACE data observed in the Pacific and Indian Ocean sectors of the ACC are consistent, with annual and semiannual amplitudes of 3.6 and 0.6 $\text{cm}_{\text{H}_2\text{O}}$ (1.1 and 0.6 $\text{cm}_{\text{H}_2\text{O}}$ with ECCO), the average over the full southern path peaks (stronger ACC) in the southern winter, on days of year 197 and 97 for the annual and semiannual components, respectively; the Atlantic Ocean annual peak is 20 days earlier. An approximate conversion factor of 3.1 Sv ($\text{Sv} \equiv 10^6 \text{ m}^3 \text{ s}^{-1}$) of barotropic transport variability per $\text{cm}_{\text{H}_2\text{O}}$ of BP change is estimated. Wind stress data time series from the Quick Scatterometer (QuikSCAT), averaged monthly, zonally, and over the latitude band 40° – 65°S , are also constructed and subsampled at the same months as with the GRACE data. The annual and semiannual harmonics of the wind stress peak on days 198 and 82, respectively. A decreasing trend over the 3 yr is observed in the three data types.

1. Introduction

The Antarctic Circumpolar Current (ACC) links the Atlantic, Pacific, and Indian Ocean basins, a 24 000-km-long current system (Olbers et al. 2004), composed of a series of filaments or fronts in temperature and salinity where most of the velocity is concentrated (Orsi et al. 1995), plus a strong eddy field. The ACC has the largest volume and mass transports (Macdonald and Wunsch 1996; Ganachaud and Wunsch 2000); it is the region where the largest time-averaged wind input is

converted to geostrophic circulation, is predominantly zonal (Wunsch 1998; Wang and Huang 2004) and balanced by pressure gradients across the bottom topography because the current has no meridional boundaries (Munk and Palmén 1951).

Modern estimates of the time-averaged volume transport of the ACC range between 120 and 157 Sv [$1 \text{ Sv} \equiv 10^6 \text{ m}^3 \text{ s}^{-1}$; Cunningham et al. (2003); Whitworth and Peterson (1985); Peterson (1988) has a long list of estimates dating back to 1933]. Many of these measurements were performed at Drake Passage. Rintoul and Sokolov (2001) estimated $147 \pm 10 \text{ Sv}$ for a line south of Australia. Ganachaud and Wunsch (2000), using various World Ocean Circulation Experiment (WOCE) cruises crossing and bounding the ACC, esti-

Corresponding author address: Victor Zlotnicki, JPL 300-323, 4800 Oak Grove Dr., Pasadena, CA 91109.
E-mail: victor.zlotnicki@jpl.nasa.gov

mated 140 ± 6 Sv at Drake Passage and 157 ± 10 Sv south of Australia. Part of the difficulty in agreeing to a time-averaged value is the fact that, although most of the time-averaged transport is baroclinic, the current does not change sign or vanish before reaching the bottom, which requires accurate deep measurements. Orsi et al. (1995) show that at most longitudes around the ACC, the transport above 3000 m, poleward of the subtropical front, is about 100 Sv. Hughes et al. (1999) offer an excellent review of theories of the mean flow dynamic balance.

The variability around this time mean has been estimated since the 1970s. Wearn and Baker (1980) used ocean bottom pressure (BP) data at two sites across Drake Passage, both around 500-m depth, with instruments replaced annually during 1976–78. They observed BP fluctuations of ~ 25 hPa on both sides of Drake Passage (with tidal contributions at the monthly and fortnightly periods of 1–2 hPa), and concluded that the geostrophic transport may vary by about 80 Sv in 1 yr if the variability were barotropic and by 31 Sv if the variability were baroclinic and retained the time-mean velocity versus depth profile. Whitworth and Peterson (1985), using a year-long (1979) deployment of moored current meters and temperature sensors, noted that most of the variability above 2500 m is barotropic, and ranged between 87 and 148 Sv with a standard deviation of 10.5 Sv. Hughes et al. (1999) estimated a 6-Sv standard deviation from the Fine-Resolution Antarctic Model (FRAM). Woodworth et al. (1996) were unsuccessful at using altimetry at Drake Passage, but clearly established (from the FRAM numerical model) that bottom pressure (what a bottom pressure gauge measures) more closely correlates with the Drake barotropic transport than the subsurface pressure (SSP—the sea level a tide gauge or satellite altimeter measures, corrected for the inverted barometer effect), anywhere around the ACC. Their maps also showed that BP or SSP south of the ACC more closely correlates with transport than do values to the north. Hughes et al. (2003) extended the comparison of BP and SSP to many gauges covering the Atlantic and Indian sectors of the ACC, and showed strong coherence in BP and SSP around Antarctica. They further verified that at subseasonal time scales transport variability is forced with undetectable time lag by time-varying circumpolar eastward winds associated with the Southern Annular Mode (SAM).

Whitworth and Peterson (1985), and most subsequent authors, now agree that while most of the time-averaged transport is baroclinic, the time variability, at least for periods less than 1 yr, is barotropic [in the same sense as in Hughes et al. (1999): a flow whose

geostrophic component has a pressure gradient independent of depth; this does not preclude Ekman and ageostrophic components]. However, estimates of baroclinic transport variability still abound (e.g., Rintoul et al. 2002; Sprintall 2003).

The relationship between wind and transport variability has also been studied extensively, with two main “branches”: comparisons with wind stress, with an implied Ekman mechanism, or with wind stress curl, with an implied Sverdrup-like mechanism. Wearn and Baker (1980) compared their 1976–78 transport estimate with gridded atmospheric pressure data from which they derived the surface wind stress. They reached several remarkable conclusions:

- 1) The BP difference across Drake Passage correlated more strongly with winds averaged over all longitudes and 45° – 65° S than with local winds.
- 2) The pressure difference spectrum was about twice as energetic as the individual spectra from the north and south sides.
- 3) The southern BP time series correlated much more strongly with the wind than the northern time series.
- 4) The BP difference time series lagged the wind by approximately 9.5 days, while the southern pressure lagged wind by 5.5 days (all approximately monthly averaged).
- 5) A simple analytical model whereby momentum input by the wind is removed by some dissipative force that increases linearly with total current momentum, with the constant an inverse time scale, and realistic values of wind stress and transport (1 dyn cm^{-2} and 124 Sv), yields a characteristic time lag of 7 days, the time it takes the wind stress or dissipation to alter significantly the ACC transport.

Peterson (1988) also noted that the southern BP at Drake Passage during 1979 correlated more strongly with the wind stress curl (averaged zonally along narrow latitudinal strips) than did the northern BP. Woodworth et al. (1996) used FRAM to map geographically the correlation coefficient of the BP against the volume transport through Drake Passage, and concluded that the southern BP “entirely encircling the Antarctic continent” shows the strongest (negative) correlation ($>90\%$) with transport changes across Drake Passage, while the BP most anywhere north of the current had zero correlation with the transport; the SSP to the north has a weaker positive correlation, and to the south it has a strong negative correlation, but it is not as clear and widespread as that for the BP.

Hughes et al. (1999) used European Centre for Medium-Range Weather Forecasts (ECMWF) wind stress and wind stress curl data, averaged over all longitudes

and different latitude bands, and BP data deployed north and south of the ACC between 1989 and 1995 in 1-yr consecutive segments, matched at the endpoints. They concluded that significant correlation existed with wind stress at least between 15- and 220-day periods (except around 60 days), that the correlation with wind stress curl was much lower than with stress, and that the correlation with the southern BPs was high, while the correlation with the northern BPs was essentially nonexistent. They saw these properties more clearly in their FRAM simulation. Gille et al. (2001) used satellite altimetry for surface transport, BP recorders at Drake Passage for barotropic transport, and winds from five different sources, and concluded that transport and wind are coherent over a range of frequencies corresponding to periods between 10 and 256 days, with barotropic transport lagging wind by ($1/8$) of a cycle at each frequency band, with higher coherence for winds on the southern side of Drake Passage. They also found that numerical models failed to reproduce the phase lag.

On time scales longer than 1 yr, Rintoul et al. (2002) found that National Centers for Environmental Prediction–National Center for Atmospheric Research (NCEP–NCAR) reanalysis wind stress and curl data local to their section, south of Australia (as opposed to zonally averaged around the ACC), were strongly correlated, and either one has at least 49% correlation with local baroclinic transport (above 2500 m) with periods >15 months, and wind leading transport by 3–10 months depending on location; their correlations in the 6–15-month band was much weaker. Meredith et al. (2004) showed that the interannual variability in Drake Passage barotropic transport over the 1980s and 1990s correlates with one version of the SAM (Thompson and Wallace 2000), a proxy for zonally averaged zonal winds. They used SSP data at a tide gauge in the Antarctic Peninsula, and compared trends in SSP for the 12 calendar months, averaged over 1990–99, with trends in the SAM similarly averaged. They noted the significance of this finding: baroclinic processes must become significant contributors to the variability of the ACC transport on longer time scales.

The observed and modeled facts that BP signals to the south of the ACC are more correlated with each other and with wind stress than with signals to the north led to simple conceptual models for the variability. Hughes et al. (1999) used both theoretical reasoning and output from the FRAM to argue that the variability in the ACC transport is dominated by a barotropic mode that follows f/h contours, that the “bottom pressure to the south of the current is a good monitor of its transport,” and that the correlation between the wind

stress to the south of Drake Passage and the overall circumpolar transport explains the correlation between the overall wind stress and transport. Aoki (2002), comparing the Southern Annular Mode index and SSP at five tide gauge stations along the Antarctic coast, corrected for short- and long-period tides, high-pass filtered all data with a cutoff of 100 days^{-1} to avoid spurious correlations induced by the seasonal cycle (Chelton 1982), and concluded that the strong negative correlation between these two quantities could be explained by a simple model whereby stronger eastward winds increase the equatorward Ekman transport, that is, a divergence of surface water near the continental margin, with the opposite consequences in the presence of a weakened eastward wind, and a response of about 1-cm change in the southern sea level per 1 m s^{-1} change in wind.

The purposes of this work are to assess whether a 3-yr time series of GRACE gravity data can add useful information to what we know about ACC variability; to add information along the large Pacific sector of the ACC, so far unsampled by tide or BP data; to take advantage of available satellite sampling by constructing spatially averaged “BP” along long segments to the south and to the north of the ACC, to assess whether north–south differences are a better measure of ACC transport than southern BP alone; and to relate this proxy for the transport variability to actual satellite-measured winds.

We first show that these observations are consistent, within their error ranges, with two different baroclinic numerical ocean models. We then show that these changes are coherent among the three basins, within their error ranges, and coherent with the zonal component of the wind stress, as directly measured by the Quick Scatterometer (QuikSCAT) satellite instrument, averaged zonally and over the band 40° – 65° S, with essentially zero lag. The unique features of this work are that for the first time we show from data that the time variability in the Pacific sector of the ACC is indeed consistent with that from the Indian sector, and to a lesser degree with the Atlantic sector, and for the first time we use time variations in the earth’s gravity field to estimate transport variability in a major current.

2. Gravity data

The key data used here are approximately monthly changes in the earth’s gravity field, measured by the GRACE satellite mission (Tapley et al. 2004). This satellite pair, currently flying at $\sim 400 \text{ km}$ height and separated by $\sim 240 \text{ km}$, measures gravity primarily by quantifying the rate of change in the distance between the two satellites to an accuracy of $\sim 1 \mu\text{m s}^{-1}$. Onboard

accelerometers help remove nongravitational accelerations, while onboard GPS receivers provide absolute position, accurate time, and the longer scales of the gravity field. Data for a period of about 30 good days need to be combined to estimate one gravity field to the desired accuracy and spatial resolution. Not all consecutive days had good data; hence, the “monthly” fields do not fall neatly into calendar months, especially in 2002–03.

This is a totally new measurement type for ocean studies; hence, it is worth reviewing its random errors, some systematic errors, and the assumptions used when applying the data to ocean circulation problems.

Water masses in the oceans, atmospheres, hydrologic basins, and ice sheets are constantly being redistributed. Time changes in the mass of a combined column of ocean and the atmosphere are reflected as time changes in ocean BP, and cause time changes in the gravity field. These very small changes in gravity can be accurately represented by changes in the mass per unit area of an

equivalent thin layer of mass (much thinner than the shortest wavelength resolved by the data) draping the surface of the earth (Wahr et al. 1998; Cazenave et al. 1999; Johnson et al. 2001). The mass per unit area can, in turn, be represented as the thickness h of an equivalent layer of water, a physically meaningful quantity related to the original cause [see Eqs. (3) and (5) below]. Here, the unit $\text{cm}_{\text{H}_2\text{O}}$ applies to such an equivalent thickness, which exerts an equivalent bottom pressure p , here described in units of $\text{cm}_{\text{H}_2\text{O}} h$ ($p = \rho gh$, with $\rho \sim 1 \text{ g cm}^{-3}$, $g \sim 9.8 \text{ m s}^{-2}$; $1 \text{ hPa} = 100 \text{ N m}^{-2} \sim 1 \text{ cm}_{\text{H}_2\text{O}}$).

The gravity field from space is represented as a spherical harmonic series, a form convenient in the orbit computations. Any quantity of the earth’s gravity field at locations outside the masses that cause it can be expressed as a sum of spherical harmonics (Heiskanen and Moritz 1967, hereinafter HM67). The gravitational potential T at colatitude θ , longitude ϕ , time t , and height H above the (spherical) surface is

$$T(\theta, \phi, t, H) = \left(\frac{GM}{a} \right) \sum_{l=0}^{\infty} \sum_{m=0}^l \left(\frac{1}{1 + H/a} \right)^l [C_{lm}(t) \cos(m\phi) + S_{lm}(t) \sin(m\phi)] P_{lm} \cos(\theta), \quad (1)$$

where G is the gravitational constant; M and a are the earth’s mass and mean radius; the dimensionless, time-varying C_{lm} and S_{lm} are called Stokes’s coefficients; and the P_{lm} are Legendre functions of degree l and order m , $m \leq l$ (see HM67 for normalization). The low degree coefficients of a reference ellipsoid are subtracted. All other quantities (gravity acceleration, deflection of the vertical, geoid height, etc.) have similar expansions whose coefficients are related to those in Eq. (1) by analytical functions of l , m and different dimensional constants. The GRACE project provides values of these C_{lm} and S_{lm} up to a maximum degree $l_{\text{max}} \sim 120$, averaged over ~ 30 days. The sum of all squared coefficients with fixed degree l can be thought of as having an associated minimum horizontal wavelength $\sim 40\,000/l \text{ km}^{-1}$.

The accuracies of the ΔC_{lm} and ΔS_{lm} from the GRACE data decrease rapidly as l and m increase around and past $40\,000 \text{ km}/H$, $H = 400 \text{ km}$, because at height H , GRACE senses an attenuated version of the gravity field at the surface, with each term in the expansion $[1/(1 + H/a)]^l$ weaker than its value at the surface of the earth [Eq. (1); in a plane geometry, the amplitude of a Fourier component with wavelength λ at height H above the surface weakens as $\exp(-H/\lambda)$]. Conversely, noise in the data at that height and wavelength increases exponentially (the inverse of this fac-

tor) as the observation is converted to a value on the earth’s surface. For different reasons, within a degree l , the error increases as order m increases. Each monthly field is the full gravity field of the earth with respect to a reference ellipsoid. We remove the average over an integer number of years, here 2003–05.

Let the surface mass density σ be the vertical integral of the density ρ through the earth’s surface layer (containing the atmosphere, the oceans, and the water–snow–ice stored on land):

$$\sigma(\theta, \phi, t) = \int_{\text{surf layer}} \rho(\theta, \phi, z, t) dz, \quad (2)$$

then time changes in $\Delta\sigma$ cause time changes ΔC_{lm} and ΔS_{lm} :

$$\Delta\sigma(\theta, \phi, t) \approx \frac{a\rho_E}{3} \sum_{l=0}^{l_{\text{max}}} \sum_{m=0}^l \frac{(2l+1)}{(1+k_l)} P_{lm}(\cos\theta) [\Delta C_{lm}(t) \cos(m\phi) + \Delta S_{lm}(t) \sin(m\phi)], \quad (3)$$

where ρ_E is the mean density of the earth and the k_l are the load Love numbers representing the deformation of the elastic lithosphere due to surface loading (Farrell 1972; Wahr et al. 1998).

The exponential increase with l in noise in the

GRACE ΔC_{lm} and ΔS_{lm} is decreased with a spatial low-pass filter $W(\theta, \varphi, \theta', \varphi')$:

$$\Delta \bar{\sigma}(\theta, \varphi) = \int W(\theta, \varphi, \theta', \varphi') \Delta \sigma(\theta', \varphi') \sin(\theta') d\theta' d\varphi', \quad (4)$$

where the W spatial function has an equivalent expansion in spherical harmonics with coefficients $W_{\text{clm}}(\theta, \varphi)$, $W_{\text{slm}}(\theta, \varphi)$. When W is only a function of the distance between (θ, φ) and (θ', φ') ,

$$\Delta \bar{\sigma}(\theta, \varphi) \approx \frac{a\rho_E}{3} \sum_{l=0}^{l_{\max}} \sum_{m=0}^l \frac{(2l+1)}{(1+k_l)} W_l P_{lm}(\cos\theta) \times [\Delta C_{lm} \cos(m\varphi) + \Delta S_{lm} \sin(m\varphi)]. \quad (5)$$

A commonly used function is a Gaussian on the sphere (Jekeli 1981; Wahr et al. 1998), whose “radius” is the distance between the center of the Gaussian and its half-amplitude point. More elaborate filters derive optimal functions W that take into account the estimated signal-to-noise ratio (Swenson and Wahr 2002b), or the striping in the data due to errors (Han et al. 2005; Swenson and Wahr 2006). Here, we use a two-step filter: first, a 500-km-radius Gaussian and, second, a simple average along a path. While the monthly solutions are given to degree and order 120, for oceanographic purposes we find the time-variable components in these first and second releases of the GRACE data are useful to degree 20–30 (wavelengths $> \sim 2000$ km) at high latitudes where the signals are strongest (see also Kanzow et al. 2005); there is useful information about stronger land hydrology signals at higher degrees.

A second set of problems arises because the GRACE satellite pairs are insensitive to the $l = 1$ coefficients, which reflect the differences between the center of mass of the earth and the origin of the coordinates; as the real fluids of the real earth move around seasonally they do induce $l = 1$ components of several millimeters in geoid height, several $\text{cm}_{\text{H}_2\text{O}}$ (Cazenave et al. 1999; Johnson et al. 2001). We experimented with an external time series from X. Wu (2005, personal communication; Wu et al. 2002) and found a slightly better match between the GRACE results and ocean models (discussed below) but decided against including it here because the series does not exist for the duration of our dataset. The coefficient $(2, 0)$, describing the equatorial bulge, showed anomalously large variability in release 01 (RL01), but the RL02 data used here closely match non-GRACE estimates (section 4).

The GRACE products are generated at three processing centers: the Jet Propulsion Laboratory (JPL), the University of Texas Center for Space Research (CSR), and the GeoForschungsZentrum Potsdam

(GFZ). JPL is responsible for “level 1” processing (a variety of essential operations starting with the downloaded raw data), and all three centers perform “level 2” processing—the conversion of level-1 GPS, range rate, accelerometer, and other data to the spherical harmonic Stokes coefficients. All centers use common background models, and so on, but each center uses different software, and each experiments with editing and processing criteria, so the resulting models are somewhat different; this encourages progress by identifying strengths and weaknesses. During the nominal month for one gravity solution, oceanic, atmospheric, and land hydrologic basins vary significantly relative to the sensitivity of the measurement. It is thus necessary to remove some model of those masses at each time step in the orbit calculation in order to minimize aliasing in the monthly fields, which can cause north–south striping errors (Han et al. 2004). Among these, tides (ocean and solid) have the most energy.

We use as input here data from the GRACE project, Jet Propulsion Laboratory (JPL) version release 02 (RL02). All RL02 data correct a variety of issues identified in RL01, including the background gravity models and various parameterizations. Among others, 1) ocean tidal dealiasing uses the Finite-Element Hydrodynamic Modeling System (FES) 2004 model; 2) there is inclusion of higher harmonics for the long-period tides; 3) a baroclinic ocean model [M. Thomas, Technische Universität (TU) Dresden, 2005, personal communication] is used to dealias fast ocean motions due to wind and pressure, including an Arctic Ocean; and 4) a pole tide correction is included (Desai 2002). This barely scratches the surface: there are numerous improvements in the relative contributions of GPS (low degrees) and intersatellite range rate (higher degrees), and so on (Bettadpur 2004; S. Bettadpur 2005, personal communication). As in RL01, the ECMWF operational monthly atmospheric masses [vertically integrated; Swenson and Wahr (2002a)] are removed over land and their wind and pressure are used to drive the TU Dresden model. Notice that, to study monthly variations in ocean mass, we must add back the monthly average of this particular ocean model to the GRACE mass fields, since the ground system attempted to remove any signal modeled by this ocean model.

When the forward problem is posed as in Eqs. (1)–(3), the answer is unique. The inverse problem is non-unique, no matter how accurate the data are: changes in the C_{lm} , S_{lm} can be caused by a variety of mass source distributions, some deep inside the earth. This is the traditional uncertainty of inverting a potential field such as gravity (e.g., Parker 1975)

The main signals from the “solid” earth in the gravity

field are body tides and postglacial rebound (PGR), with very different time scales. At any one location, the PGR signal behaves like a linear trend in time; hence, such trends must be viewed with caution. A second issue arises from the contamination of larger nearby signals in the inversion: ocean signals are much smaller than land signals, and the 500-km Gaussian average of a small oceanic signal within, say, 500 km of a large continental signal, will not be retrievable simply because the tail of the Gaussian averaging kernel will include the large land signal at the ocean point. Thus, to first approximation, we must disregard ocean estimates within one to two averaging radii of large land signals.

The actual data used here cover January 2003–November 2005, except June 2003 and July–October 2004, a total of 30 nominal months. The missing months occur because the ground track drifts slowly and goes through near-exact repeats during which there is not enough ground coverage to define a monthly field to sufficient resolution. Some days within the available months are missing (see the GRACE Web site: <http://grace.jpl.nasa.gov>). Data collection started in April 2002, but the satellite software was reconfigured several times during 2002 so as to remove detected problems; hence, the 2002 data are of somewhat lower quality and are not used here.

3. BP data–model consistency and formal errors

Given the above caveats, the actual data results are much more reasonable than one might fear. We first compare GRACE “BP” with BP time series from two numerical models: (a) the JPL version of the Estimating the Circulation and Climate of the Ocean (ECCO) model–assimilation system, which assimilates sea surface topography from the Ocean Topography Experiment (TOPEX)/Poseidon and *Jason* altimeters and XBT data (Kim et al. 2004), and (b) a mass-conserving version of ROMS (Song and Hou 2005; Song and Zlotnicki 2004) with no data assimilation. Both models are forced by NCEP–NCAR reanalysis winds and fluxes; neither includes atmospheric pressure forcing. The ECCO run covers the GRACE data period, but the ROMS–Song run ends in early 2004. The GRACE data are presmoothed with the 500-km Gaussian, then averaged along the paths shown in Fig. 1. ECCO has 1° resolution at high latitudes, while the ROMS/SONG model has $\sim\frac{1}{3}^\circ$ resolution in latitude and 0.5° resolution in longitude. ECCO was *not* presmoothed to match the GRACE data; the ROMS/SONG model data were presmoothed to match ECCO, then both ECCO and ROMS values were averaged along the same paths as the GRACE data. The spatial averages at fixed times of the ECCO, ROMS, and GRACE grids over the global

oceans for each “month” were removed: all three “datasets” conserve global ocean mass at all times. The reasons are different: the Massachusetts Institute of Technology (MIT) model underlying ECCO (Marshall et al. 1997) conserves volume, not mass, and no net mass flux into or out of the oceans is included in the forcing, hence the need to remove the globally averaged mass change (Greatbatch et al. 2001); the ROMS model does not suffer from this deficiency, but the NCEP–NCAR fluxes forcing it are suspect; and the GRACE monthly changes in mass over the global oceans do reflect the real world’s seasonal changes among ocean, land, and cryospheric reservoirs (Minster et al. 1999; Chambers et al. 2004) but they are removed for consistency with the other two. Last, a fourth model output is included in the plots below: the monthly and spatial average of the TU Dresden model used to dealias the GRACE data in ground processing; it must be reemphasized that the mass predicted by this model was removed from the GRACE signal during ground processing four times daily; hence, it is necessary to add back its monthly average to the GRACE data.

Figure 1 shows three time series for a choice of north and south paths bracketing the ACC in the Pacific. The averaging paths are shaded in Fig. 1a; the center of the strip has maximum Gaussian weight, and the north and south edges of the strip have $\frac{1}{2}$ the maximum weight. Figure 1d shows the difference in the time series along the northern path minus the time series along the southern path. For this time series, GRACE observes signals with standard deviation (std dev) of 3.40 $\text{cm}_{\text{H}_2\text{O}}$ (first row at the bottom of Fig. 1d), while ECCO indicates a weaker 1.80 $\text{cm}_{\text{H}_2\text{O}}$ std dev, and ROMS indicates a 2.37 $\text{cm}_{\text{H}_2\text{O}}$ std dev. Assume for a moment that the ECCO or ROMS numerical model outputs are data of unknown quality, and we are trying to assess this new data type, GRACE. The correlation between ECCO and ROMS (68%, written on the second line at the bottom of the panel) and the std dev difference between the two models over their common time span (1.74 $\text{cm}_{\text{H}_2\text{O}}$) give an idea of their combined uncertainty. The correlations between GRACE and ECCO (89%) and between GRACE and ROMS (50%) suggest that ECCO is closer to “reality.” The difference GRACE–ECCO has a 2.00 $\text{cm}_{\text{H}_2\text{O}}$ std dev, higher than the std dev of ECCO (1.80 $\text{cm}_{\text{H}_2\text{O}}$) but lower than the std dev of GRACE (3.40 $\text{cm}_{\text{H}_2\text{O}}$). On the one hand, this repeats what the high correlation coefficient already told us. But the variance of the difference is a much more sensitive indicator of “accuracy.” The 2.00 $\text{cm}_{\text{H}_2\text{O}}$ std dev difference of GRACE–ECCO is one measure of the combined uncertainty in both ECCO and GRACE, which places an upper bound on the uncer-

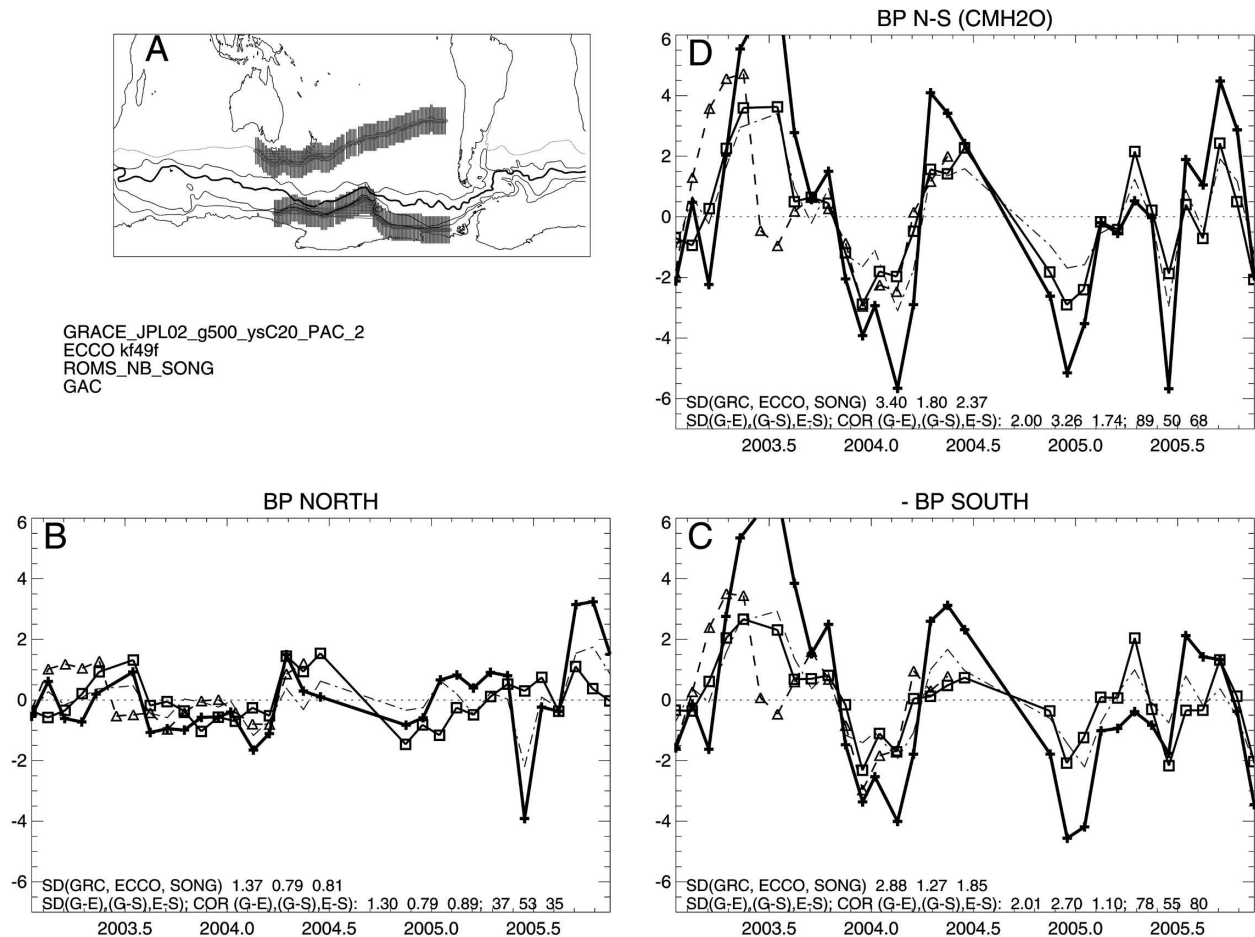


FIG. 1. (a) Map showing ACC fronts from Orsi et al. (1995), thick black line is the polar front, with the location of the Pacific sector's northern and southern paths (shaded) over which the GRACE data and model output were averaged. (b) The BP time series averaged over the northern path: black/solid/thick/crosses, GRACE; black–solid–thin–squares, ECCO ocean model; gray–dashed–thin–triangles, ROMS/SONG model; and gray–dot–dash from the TU Dresden model used to dealias GRACE. Vertical axis units: $\text{cm}_{\text{H}_2\text{O}}$. Horizontal axis units: yr. The upper of two lines at the bottom of the plot, starting with “SD,” lists the std devs of the GRACE, ECCO, and ROMS (labeled SONG) time series, respectively. The lower SD line lists the std devs of the (GRACE–ECCO), (GRACE–ROMS), and (ECCO–ROMS) time series. The next three numbers are the corresponding correlation coefficients expressed as percent. (c) Time series as in (B) for the southern box, but with sign reversed for easier comparison with (d). (d) Time series differences, northern–southern (>0 implies increased ACC transport).

tainty of the GRACE BP, because these are truly independent estimates of the same quantity. Their high correlation (89%) is in part dominated by the seasonal cycle, but if the phase were not the same, the correlation would decrease significantly. (In all these correlations, with 30 independent samples, values greater than 37% are different from zero at the 95% level, and values above 47% at the 99% level.) ECCO and ROMS have the same NCEP–NCAR forcing, both lack pressure forcing, so they have common errors, and their std dev difference is a lower bound on their combined error.

Figures 1b and 1c show the time series averaged along the northern path and along the southern path,

with the sign of the BP changed, respectively. Most of the signal in the north–south difference comes from the southern time series, as the northern one is much weaker, and does not show the seasonal signal present in the southern time series. The small numbers at the bottom of each panel in Fig. 1 show a peculiar property: correlation between GRACE and ECCO is 78% for the southern path, with a $2.01 \text{ cm}_{\text{H}_2\text{O}}$ std dev difference; the corresponding quantities for the difference between the north and south are 89% and $1.96 \text{ cm}_{\text{H}_2\text{O}}$. This is so even though GRACE and ECCO seem to be essentially uncorrelated along the weak, northern path (35% correlation). The most likely explanation for this behavior is the errors in GRACE, which have a north–

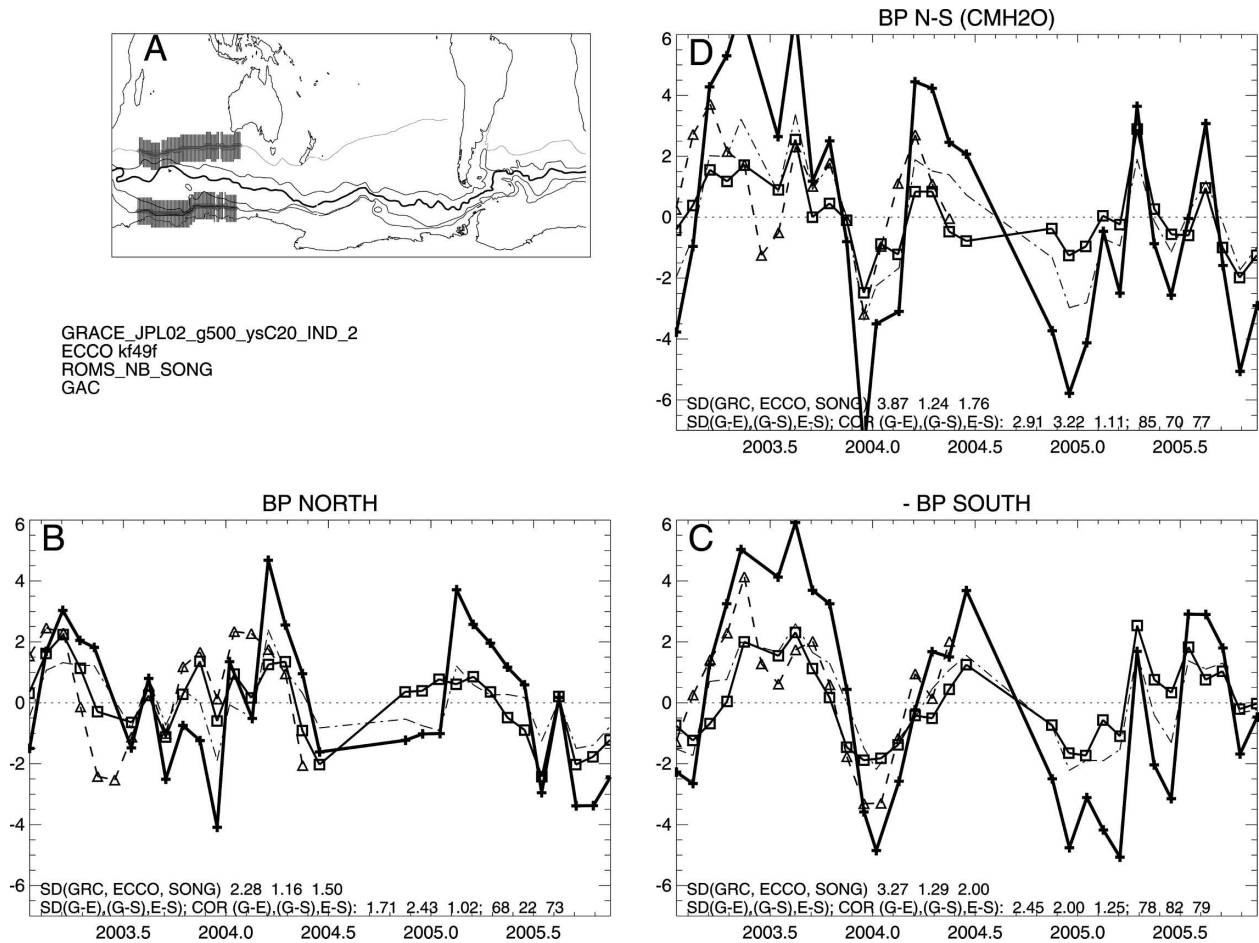


FIG. 2. Same as in Fig. 1 but for the Indian Ocean.

south correlation, minimized by differencing the north-south paths, especially the absence of the two coefficients of degree 1.

Figures 2 and 3 are equivalent to Fig. 1 except for the Indian and Atlantic Ocean sectors, respectively. There are common elements among Figs. 1–3: the southern time series always has the strongest signal (larger std dev), and a clearly defined seasonality, with a maximum around midyear in all three basins for all 3 yr. The northern time series, in addition to being weaker, do not have a common seasonality, and do not appear to be correlated (see Meredith and Hughes 2004).

The southern and north-south time series correlate well among basins because their seasonal cycles peak at about the same time of year (see also Chelton 1982). After removing annual and semiannual sinusoids from all time series, we find that the southern series for the Pacific and Indian Oceans have 27% (GRACE) or 55% (ECCO) correlation, while the correlation between the Pacific and Atlantic series is 7% for both. We will return later to the fact that the Atlantic time series for

both GRACE and ECCO differ from the Pacific and Indian series. When the north-south differences are used, instead of the south only, the correlations for the Pacific and Indian and Pacific and Atlantic Oceans rise to 63% and 44% for GRACE and 54% and 24% for ECCO.

Because neither the ECCO nor ROMS BPs have associated error estimates, we use their difference as a measure of their uncertainty: the north or south time series differ between the two models, with std dev values ranging between 1.2 and 2.7 $\text{cm}_{\text{H}_2\text{O}}$, with a quadratic mean of 1.5 $\text{cm}_{\text{H}_2\text{O}}$. Assuming equal errors (even though GRACE agrees with ECCO most often) gives an error to the modeled north or south BP of $\sim 1.0 \text{ cm}_{\text{H}_2\text{O}}$. The differences between GRACE and ECCO ranged between 1.3 and 2.7 $\text{cm}_{\text{H}_2\text{O}}$, with a quadratic mean of 2.0 $\text{cm}_{\text{H}_2\text{O}}$; assuming that it is the sum of the 1.0 $\text{cm}_{\text{H}_2\text{O}}$ error in ECCO and the GRACE error, and that these are uncorrelated, gives an approximate error for the GRACE path averages of 1.7 $\text{cm}_{\text{H}_2\text{O}}$ (this, of course, depends on the length of the path; the Pacific

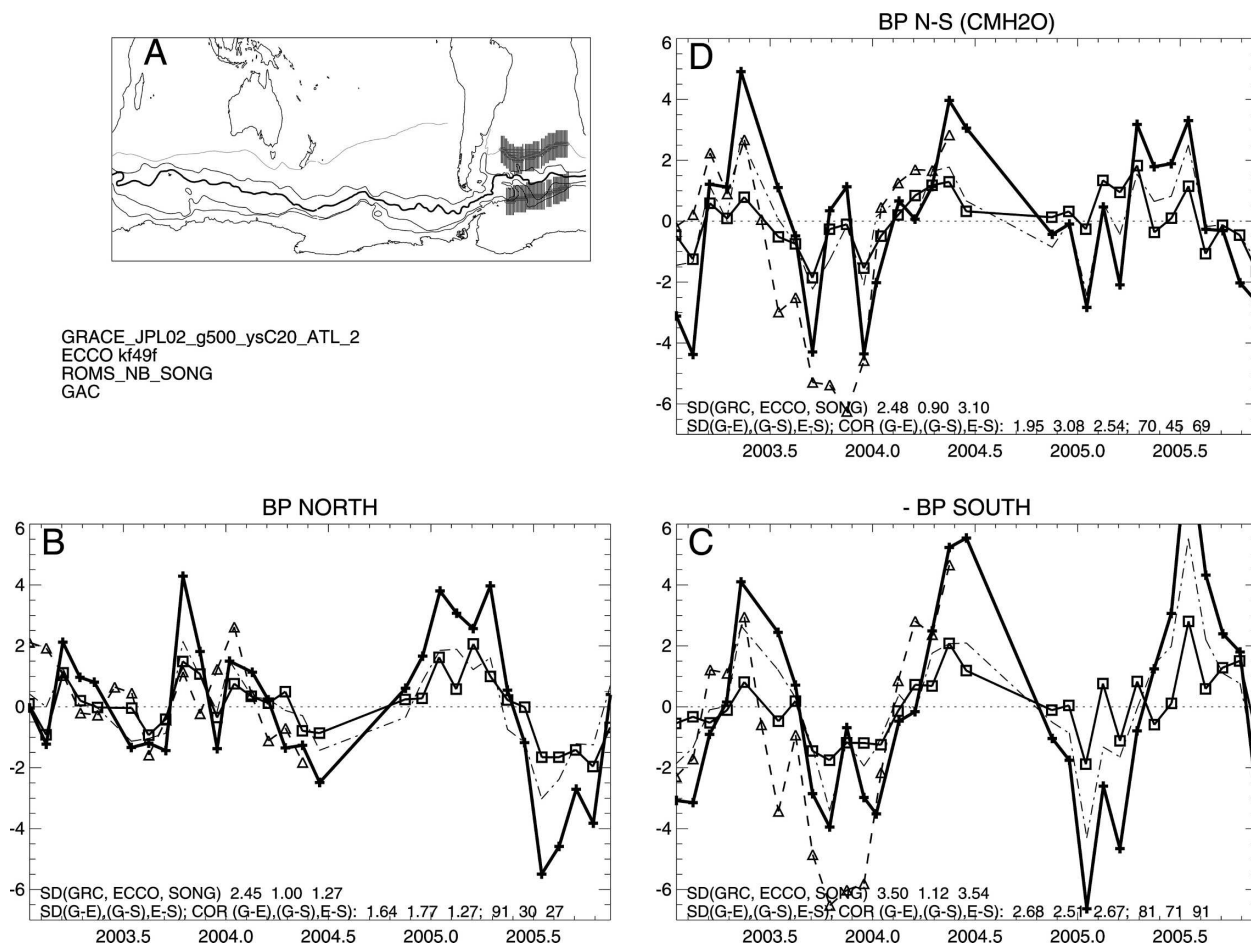


FIG. 3. Same as in Fig. 1 but for the Atlantic Ocean.

paths are longer and indeed have smaller std dev differences from ECCO).

We also present a different way to assess the error in the GRACE BPs. 1) The GRACE project provides formal noise estimates with each set of monthly spherical harmonic coefficients, based on the propagation of variances through the least squares estimation of the gravity field, followed by a “calibration” procedure so that the total variance better agrees with the discrepancy estimates from other sources. 2) There is a pre-launch shape to the noise error curve as a function of degree and order, based on simulations. The “official” set of calibrated noise for each $\Delta C_{lm}(t)$, $\Delta S_{lm}(t)$ is available online (<http://podaac.jpl.nasa.gov/grace>). Here, we use a slightly different calibration of the formal noise. Wahr et al. (2004, 2006) estimated an upper bound on the accuracy of a single 750-km Gaussian average as 2.1 $\text{cm}_{\text{H}_2\text{O}}$ std dev (1.5 $\text{cm}_{\text{H}_2\text{O}}$ for a single 1000-km Gaussian average) based on the assumption that at any location, all of the GRACE signal that was not an annual cycle must be noise. Assuming that the shape of the

prelaunch noise curve is maintained, then multiplied by 40, the root sum square (degree variances) of the noise variances yield the same value as the scaled residual from the annual cycle. Since these residuals from the annual cycle have a Gaussian probability distribution, one can assert that about 68% of the true values lie within ± 1 standard deviation of the estimated value.

Using method 2 above, with m -dependent errors, and propagating the noise variances in the gravity coefficient through the conversion to the mass distribution and the two-step filters described above (Swenson and Wahr 2002b), we obtain error values for the BPs, with the following general characteristics: the northern paths used here have calibrated errors ranging between 1.02 and 1.05 $\text{cm}_{\text{H}_2\text{O}}$, the southern paths have calibrated errors between 0.95 and 0.97 $\text{cm}_{\text{H}_2\text{O}}$, and the differences have errors between 1.1 and 1.3 $\text{cm}_{\text{H}_2\text{O}}$. In general, the GRACE noise decreases with increasing latitude, because GRACE tracks become closer to each other; also the noise in the north–south difference is smaller than would be obtained by adding in quadrature those in the

northern and southern paths, perhaps because the tails of the Gaussian averages overlap slightly. This $1.0 \text{ cm}_{\text{H}_2\text{O}}$ noise due to data noise underestimates the $1.7 \text{ cm}_{\text{H}_2\text{O}}$ error obtained above. A different source of GRACE error derives from the leakage of real oceanic or continental signals outside the paths. The Gaussian smoother has weight = 1 at the origin, 0.5 at 500 km, and 0.1 at 900 km: the southern path is prone to leakage from the Antarctic continent. An estimate of leakage was obtained from the standard deviations of the spatially filtered monthly mass anomalies north and south of the path edges, weighted by the filter value; only values 500 and 1000 km away were included, and added in quadrature. These estimates range between 0.8 and $1.3 \text{ cm}_{\text{H}_2\text{O}}$ for the northern paths (highest in the Atlantic), and between 1.6 and $1.8 \text{ cm}_{\text{H}_2\text{O}}$ for the southern paths. This leakage is not random noise and probably has a strong seasonal signal. Since the most important source is the Antarctic continent, whose mass variability can only be determined from GRACE itself, we simply list this as an error. The final error estimate is the quadrature sum of the noise and leakage components for each path. In general, the northern paths have total errors $\sim 1.4 \text{ cm}_{\text{H}_2\text{O}}$, while the southern ones are $1.9 \text{ cm}_{\text{H}_2\text{O}}$.

In summary, the accuracy of the BP estimates averaged along these paths ranges between 1.7 (from the discrepancy with numerical models) and $1.9 \text{ cm}_{\text{H}_2\text{O}}$ based on the formal error propagation.

4. Relation to wind

The seasonal cycle in the transport variability during 2003–05, as measured by a drop in the southern BP, of ± 4 to $\pm 5 \text{ cm}_{\text{H}_2\text{O}}$, is well captured by the GRACE data in all three basins, in general agreement with the independent ECCO model. Figure 4 shows the BP averaged along the full southern path, including all three basins, with the eastward component of wind stress averaged over 1 month, the latitude band 40° – 65°S , and all longitudes superimposed. The latitude band chosen is where the wind remains strong, always eastward on the monthly averages, and close to the surface expression of the SAM index. The data are direct measurements from the SeaWinds instrument on the QuikSCAT satellite [Chelton and Freilich (2005), with the Smith (1988) conversion from neutral wind to stress]. These winds differ from the NCEP–NCAR reanalysis forcing used by the numerical models here, making the squared coefficients that are compared quite independent. The figure also includes plots of the annual and semiannual fits to the BP and wind data (using only those months when GRACE data exist) and lists their phase (defined

as the day of year when the cosine is at its maximum). The fits place the maxima of the wind and GRACE BP at the annual frequency on days 198 and 197, respectively, and those at the semiannual frequency at days 82 and 97. The differences are negligible, given the monthly averaging of the data, the fact that GRACE data are not defined every month over the 3-yr period, that on a particular month the data may be biased toward the beginning or end of the month, etc. ECCO places the maxima on days 185 and 90, respectively.

A second property of the relationship between the southern BP and wind is apparent in the GRACE time series in Fig. 4: a downward trend of $-1.2 \text{ cm}_{\text{H}_2\text{O}} \text{ yr}^{-1}$ [$-1.0 \text{ cm}_{\text{H}_2\text{O}} \text{ yr}^{-1}$ using the C_{20} coefficient from Cheng and Tapley (2004)]. ECCO data also show a downward trend, albeit a factor of 5 smaller: $-0.2 \text{ cm}_{\text{H}_2\text{O}} \text{ yr}^{-1}$, as does the wind time series at $-2.7 \times 10^{-3} \text{ N m}^{-2} \text{ yr}^{-1}$. Thompson and Solomon (2002) documented a 30-yr trend toward the high-index polarity in the SAM, toward stronger winds. Superimposed on this trend, there is variability with shorter time periods, especially 2–5 yr (information online at <http://www.cpc.noaa.gov/products>). Since about 1998, the index has been on a downward trend, which is captured by the QuikSCAT wind data (available since 1999). The extent to which the ACC weakens as the wind does over a few years contains useful information on what controls interannual ACC variability.

Trends in mass measured by GRACE, especially near Antarctica, North America, or Asia, should first be thought of as being caused by postglacial rebound [PGR, or glacial isostatic adjustment; for Antarctica in particular, see Velicogna and Wahr (2006)]. The two key components of a PGR model are the ice load history and the mantle viscosity profile. We used the ICE-5G deglaciation model of Peltier (2004) and a mantle model similar to the one he used to construct ICE-5G, that is, a 90-km-thick elastic lithosphere overlying the upper and lower mantles with 0.9 and $3.6 \times 10^{21} \text{ Pa s}$ viscosities, respectively. The PGR gravity signal (not the landmass vertical displacement) was converted to $\text{cm}_{\text{H}_2\text{O}}$ and smoothed with a 700-km-radius Gaussian (the difference from the 500-km Gaussian used elsewhere in this work is of second order). We estimate the rate of rebound along the full southern path (Fig. 4) as $0.04 \text{ cm}_{\text{H}_2\text{O}} \text{ yr}^{-1}$. Within reasonable extremes in the uncertainty of the viscosity profile, the average rate cannot exceed $0.13 \text{ cm}_{\text{H}_2\text{O}} \text{ yr}^{-1}$. This trend must be subtracted from our trend, increasing its magnitude. However, since it is over an order of magnitude smaller than $-1.2 \text{ cm}_{\text{H}_2\text{O}} \text{ yr}^{-1}$, we conclude that PGR is not a main contributor to the observed trend. A second source of an unrealistically large GRACE trend may be

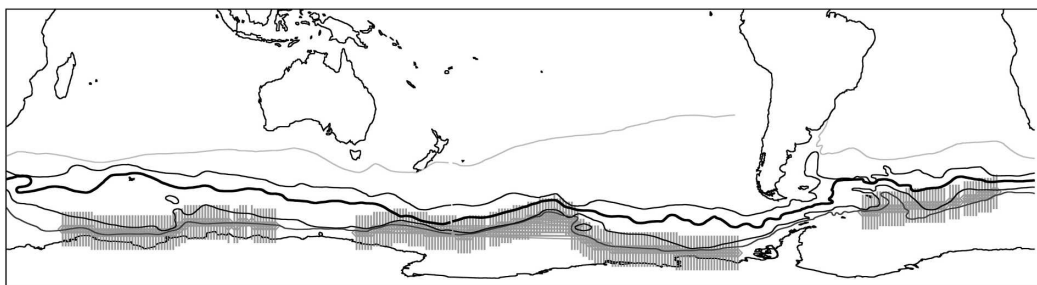
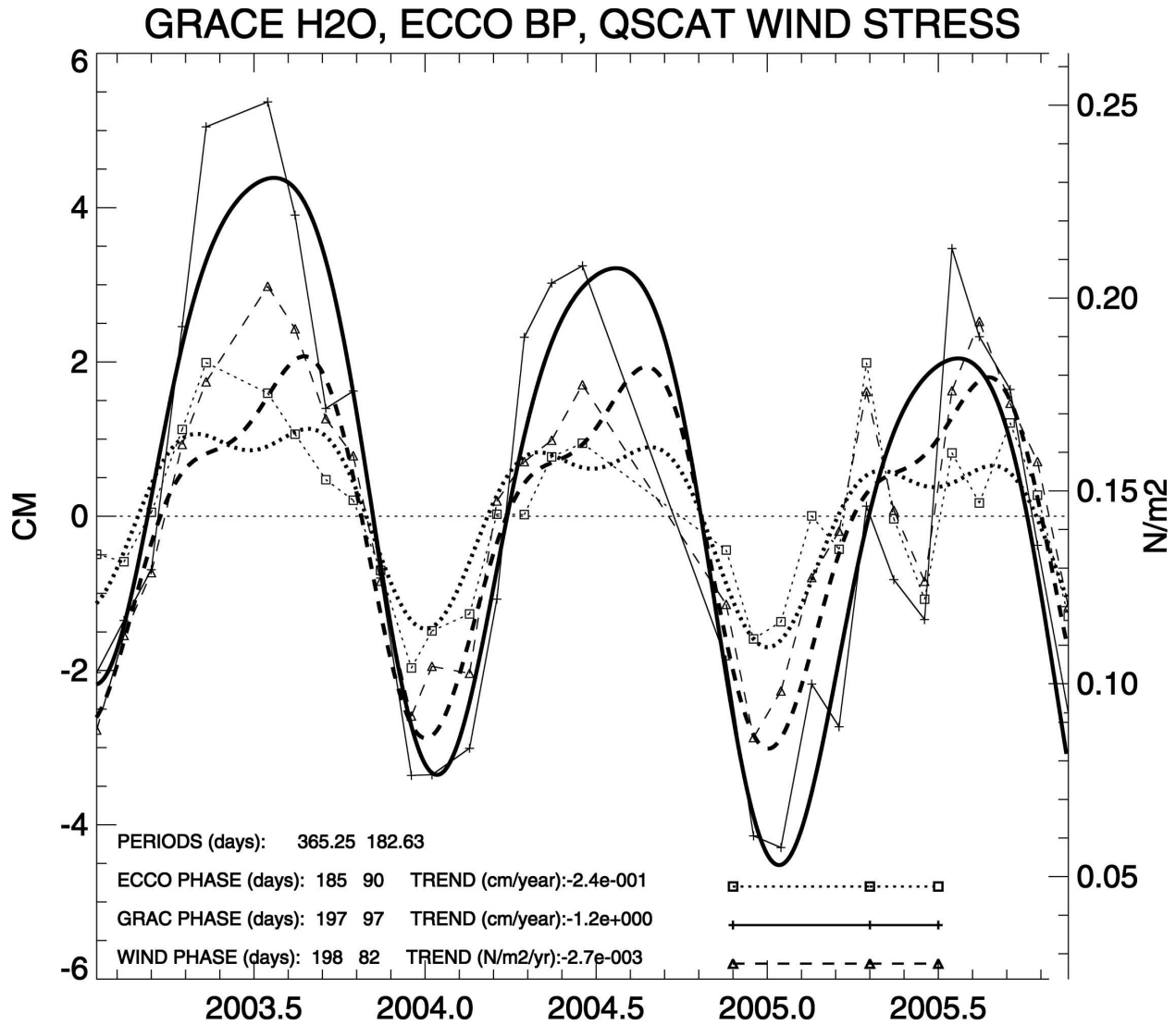


FIG. 4. (top) Solid–thin line–crosses: BP averaged over the southern path (shaded in the map below) from GRACE data, scale on the left axis. Dotted–thin line–squares: same as above but from the ECCO model. Dashed–thin line–triangles: wind stress, averaged as indicated in the text, scale on the right axis. Thin, ragged lines: actual data at GRACE sampling times. Thick, smooth lines: annual plus semiannual harmonic fit to the respective data (solid, GRACE; dotted, ECCO; dashed, wind). (bottom) The overall path along which the spatial averages are obtained, including segments from the Indian, Pacific, and Atlantic basins.

the aliasing of uncertainties in the K_2 tide [alias period ~ 4 yr; Knudsen (2003); K.-W. Seo (2006, personal communication)].

5. Barotropic transport

The geostrophic component of the barotropic transport across a section between two horizontal positions a and b , in the squared coefficients of a sea surface height change, is (Hughes et al. 1999)

$$T_g = \int_a^b \frac{gH}{f} \frac{\partial H}{\partial s} ds. \quad (6)$$

One can disregard the change in g ($< 1/300$), but the changes in H/f are large over the paths here: the ratio $H/\sin(\phi)$ along the northern paths divided by the same ratio for the southern paths ranges between 2 (Pacific) and 1.4. When a and b are not connected by a path of constant H/f , the relationship between the transport and pressure depends on the path of the current itself, which can change in time. Hence, following are crude estimates of the total transport variability. If the whole path of integration did lie on the same contour of H/f , then one could compute the volume transport variation as

$$T = (gH/f)\Delta h, \quad (7)$$

where Δh is the water height equivalent of the BP change. All the paths discussed here have depths between 4000 and 4700 m, taking a nominal latitude of 60°S , and by using Eq. (7) the time changes in horizontal pressure would be equivalent to $3.1 \text{ Sv} (\text{cm}_{\text{H}_2\text{O}})^{-1}$ change in BP. For comparison, Meredith et al. (1996) estimated $2.3\text{--}2.7 \text{ Sv} (\text{cm}_{\text{H}_2\text{O}})^{-1}$ at the shallower depths in Drake Passage, while Hughes et al. (1999) gave a model-derived value of H/f (their Fig. 5) that corresponds to $\sim 3\text{--}3.7 \text{ Sv} (\text{cm}_{\text{H}_2\text{O}})^{-1}$, and Hughes et al. (2003) regressed the model transport to BPR and altimetry data, resulting in 1.2 and $2.1 \text{ Sv} (\text{cm}_{\text{H}_2\text{O}})^{-1}$, respectively. Given the imperfect correlation between the model and real transports, the latter probably are underestimates. This reasoning still requires a change in BP [Δh in Eq. (7)], which assumes zero change related to ACC variability along the northern path.

Thus, the variability at the annual and semiannual periods in Fig. 4, $3 \text{ cm}_{\text{H}_2\text{O}}$, would imply 9 Sv with an uncertainty of $\pm 5.6 \text{ Sv}$.

6. Discussion

We used 30 monthly estimates of BP from the GRACE and ECCO datasets, and 30 monthly estimates of zonally averaged wind stress from QuikSCAT satellite data, spanning 2003–05. The long zonal averages are important in reducing GRACE noise (Han et al. 2004). The GRACE data are generally consistent

with the ECCO model used for comparison in the ACC region: they have high correlation, although in absolute numbers, the GRACE estimate of BP is about twice as strong as ECCO's. These two "data" sources are completely independent, and the signals relatively small ($\pm 4 \text{ cm}_{\text{H}_2\text{O}}$ in GRACE), which makes the agreement all the more remarkable. The GRACE error we estimate for the path averages is between ± 1.7 and $\pm 1.9 \text{ cm}_{\text{H}_2\text{O}}$. Given our rough conversion of $3.1 \text{ cm}_{\text{H}_2\text{O}} \text{ Sv}^{-1}$, these values as $\pm 5.3\text{--}5.9 \text{ Sv}$ uncertainties in barotropic transport.

We found that the phase estimates were sensitive to reasonable changes in the choice of averaging path. This is understandable for the southern paths especially, as erring too far north includes the ACC itself in the average, and erring too far south brings in seasonal signals from the Antarctic continent. With that caveat, the general observation that BP north of the ACC is weak and uncorrelated both among basins and with the wind is confirmed here, as is the observation that BP south of the ACC correlates well among the three basins and with the wind. However, we also noticed that the GRACE data matched the ECCO output better in the north–south differences than in the southern time series alone. This we attribute to residual errors in GRACE due to the absence of the degree-1 coefficients. This error has about 1.2-cm amplitude in the annual sinusoid along the overall southern path, peaking near day 220, which is clearly not negligible. The error is much smaller in the north–south difference, because both paths have about the same phase and amplitude. Chambers (2006) and Chambers et al. (2004) chose to add a climatological annual sinusoid of these degree-1 terms based on non-GRACE data. We decided to leave this component out and call it a systematic error in our analysis.

The phase of the maximum in the annual cycle in BP from the GRACE data averaged along all the southern paths (day 197) is within 1 day of the maximum in the QuikSCAT wind (day 198). For the semiannual cycle, the GRACE and QuikSCAT data put the maxima at days 97 and 82, respectively, a 15-day difference. Given the 30-day-averaged data, the missing months, and the missing data within certain months, these differences in phase are statistically indistinguishable from zero. The amplitudes of the annual and semiannual cycles are 3.6 and $0.6 \text{ cm}_{\text{H}_2\text{O}}$ for GRACE and 1.1 and $0.5 \text{ cm}_{\text{H}_2\text{O}}$ for ECCO. These translate roughly to 11 and 2 Sv for GRACE and 4 and 1.8 Sv for ECCO, at the respective frequencies. Whether this release of GRACE data is calibrated "too high," or the ECCO model is too sluggish in the ACC region, or both, are topics for future work.

A puzzling feature of this analysis is that while the Pacific and Indian Ocean southern signals are in good agreement, the Atlantic annual phase in our results occurs about 20 days earlier than in the Pacific or Indian Oceans. This is true in both the ECCO simulation and the GRACE data. Furthermore, the semiannual maximum in the Atlantic time series is wildly off from the other two basins (60 days, but later in GRACE and earlier in ECCO). The Atlantic path is the shortest, and the one permitting the least amount of noise reduction, which may be part of the explanation. We moved the southern path northward and southward with limited success. A second possible reason is other circulation sources in the large Weddell Sea, south of the southern boundary of the ACC, influencing the estimate. This is puzzling, as Hughes et al. (2003) found consistency between the Atlantic and Indian Ocean sectors, using gauges in the Antarctic Peninsula, nearby islands, and in the Weddell Sea.

We believe the decreasing trends in the strength of the ACC suggested by GRACE data, modeled by ECCO, and apparently driven by weakening winds are real. Clearly they are not a result of PGR. The magnitude of the GRACE trend, however, is too large, a data artifact possibly due to tidal aliasing (the value of this trend is closer to that of ECCO when using the CSR release-01 data but using a non-GRACE source for the degree-2 coefficient). It is tempting to do a small sensitivity exercise on the seasonal (annual) scale and the 3-yr trends, assuming that forcing in one frequency band causes a response in the same band. This is clearer in units of wind speed rather than stress. The eastward monthly wind ranges between 5.0 and 11.1 m s^{-1} , while its annual plus semiannual harmonics range between 7.3 and 10.4 m s^{-1} . Thus, if the 3.2 m s^{-1} range in annual plus semiannual wind harmonics drive the 6.15 $\text{cm}_{\text{H}_2\text{O}}$ range in the annual plus semiannual GRACE BP harmonics, the sensitivity is approximately 2 $\text{cm}_{\text{H}_2\text{O}} (\text{m s}^{-1})^{-1}$. The corresponding sensitivity for ECCO would be 0.9 $\text{cm}_{\text{H}_2\text{O}} (\text{m s}^{-1})^{-1}$ [closer to Aoki's (2002) 1 $\text{cm}_{\text{H}_2\text{O}} (\text{m s}^{-1})^{-1}$]. For the 3-yr trend, however, the sensitivity is significantly higher because the wind trend is so small: even using ECCO the ratio would be 5 $\text{cm}_{\text{H}_2\text{O}} (\text{m s}^{-1})^{-1}$. This difference in sensitivity points to a different mechanism, or at least a different form of equivalent friction, at these two time scales (see also Hall and Visbeck 2002).

The data used here are from the second release from the GRACE project, as processed at JPL. This version corrects a number of identified weaknesses in the first release. For example, the results from this dataset are quantitatively different from the results using the first release: the phases of the annual cycle shift by about 10

days, the amplitude of the annual cycle using the first CSR release is weaker, and so on. One can be certain that better results will be derived from the next release of the same data, longer time series, and cleaner estimates of the degree-1 terms from other sources.

Acknowledgments. This manuscript benefited from many discussions with M. Watkins (JPL) and S. Bettadpur (U. Texas). Very helpful reviews were provided by C. Hughes and K. Speer. QuikSCAT data are produced by Remote Sensing Systems (available online at www.remss.com) and sponsored by the NASA Ocean Vector Winds Science Team. This work was performed in part at the Jet Propulsion Laboratory, California Institute of Technology, under contract with the National Aeronautics and Space Administration. The work was sponsored by NASA's GRACE Science Team, the Physical Oceanography program, and Earth Science REASoN. We thank Drs. Eric Lindstrom, John Labrecque, and Martha Maiden for their support. The lead author (VZ) greatly benefited from C. Wunsch's professional and personal example. On the latter, VZ has not forgotten the time after graduating and moving away from MIT when he, his wife Diana, and their young baby had just visited Carl's home in Cambridge and then headed for Logan Airport—without the airplane tickets. By the time the travelers noticed, and called Carl's home, he had arrived at Logan, tickets in hand.

REFERENCES

- Aoki, S., 2002: Coherent sea level response to the Antarctic Oscillation. *Geophys. Res. Lett.*, **29**, 1950, doi:10.1029/2002GL015733.
- Bettadpur, S., 2004: Level-2 gravity field product user handbook. GRACE 327–734, University of Texas, Austin, TX, 17 pp.
- Cazenave, A., F. Mercier, F. Bouille, and J.-M. Lemoine, 1999: Global-scale interactions between the solid Earth and its fluid envelopes at the seasonal time scale. *Earth Planet. Sci. Lett.*, **171**, 549–559.
- Chambers, D. P., 2006: Observing seasonal steric sea level variations with GRACE and satellite altimetry. *J. Geophys. Res.*, **111**, C03010, doi:10.1029/2005JC002914.
- , J. Wahr, and R. S. Nerem, 2004: Preliminary observations of global ocean mass variations with GRACE. *Geophys. Res. Lett.*, **31**, L13310, doi:10.1029/2004GL020461.
- Chelton, D. B., 1982: Statistical reliability and the seasonal cycle—Comments on “Bottom pressure measurements across the Antarctic Circumpolar Current and their relation to the wind.” *Deep-Sea Res.*, **29A**, 1381–1388.
- , and M. H. Freilich, 2005: Scatterometer-based assessment of 10-m wind analyses from operational ECMWF and NCEP numerical weather prediction models. *Mon. Wea. Rev.*, **133**, 409–429.
- Cheng, M., and B. D. Tapley, 2004: Variations in the Earth's ob-

- lateness during the past 28 years. *J. Geophys. Res.*, **109**, B09402, doi:10.1029/2004JB003028.
- Cunningham, S. A., S. G. Alderson, B. A. King, and M. A. Brandon, 2003: Transport and variability of the Antarctic Circumpolar Current in Drake Passage. *J. Geophys. Res.*, **108**, 8084, doi:10.1029/2001JC001147.
- Desai, S. D., 2002: Observing the pole tide with satellite altimetry. *J. Geophys. Res.*, **107**, 3186, doi:10.1029/2001JC001224.
- Farrell, W. E., 1972: Deformation of the Earth by surface loads. *Rev. Geophys. Space Phys.*, **10**, 761–797.
- Ganachaud, A., and C. Wunsch, 2000: Improved estimates of global ocean circulation, heat transport and mixing from hydrographic data. *Nature*, **408**, 453–457.
- Gille, S. T., D. P. Stevens, R. T. Tokmakian, and K. J. Heywood, 2001: Antarctic Circumpolar Current response to zonally averaged winds. *J. Geophys. Res.*, **106**, 2743–2759.
- Greatbatch, R. J., Y. Lu, and Y. Cai, 2001: Relaxing the Boussinesq approximation in ocean circulation models. *J. Atmos. Oceanic Technol.*, **18**, 1911–1923.
- Hall, A., and M. Visbeck, 2002: Synchronous variability in the Southern Hemisphere atmosphere, sea ice, and ocean resulting from the annular mode. *J. Climate*, **15**, 3043–3057.
- Han, S.-C., C. Jekeli, and C. K. Shum, 2004: Time-variable aliasing effects of ocean tides, atmosphere, and continental water mass on monthly mean GRACE gravity field. *J. Geophys. Res.*, **109**, B04403, doi:10.1029/2003JB002501.
- , C.-K. Shum, C. Jekeli, C. Y. Kuo, C. Wilson, and K. W. Seo, 2005: Non-isotropic filtering of GRACE temporal gravity for geophysical signal enhancement. *Geophys. J. Int.*, **163**, 18–25.
- Heiskanen, W. A., and H. Moritz, 1967: *Physical Geodesy*. W. H. Freeman and Co., 364 pp.
- Hughes, C. W., M. P. Meredith, and K. J. Heywood, 1999: Wind-driven transport fluctuations through Drake Passage: A southern mode. *J. Phys. Oceanogr.*, **29**, 1971–1992.
- , and Coauthors, 2003: Coherence of Antarctic sea levels, Southern Hemisphere annular mode, and flow through Drake Passage. *Geophys. Res. Lett.*, **30**, 1464, doi:10.1029/2003GL017240.
- Jekeli, C., 1981: Alternative methods to smooth the Earth's gravity field. Geodetic Science and Survey Rep. 327, The Ohio State University, Columbus, OH, 48 pp.
- Johnson, T. J., C. R. Wilson, and B. F. Chao, 2001: Non tidal oceanic contributions to gravitational field changes: Predictions of the Parallel Ocean Climate Model. *J. Geophys. Res.*, **106**, 11 315–11 334.
- Kanzow, T., F. Flechtner, A. Chave, R. Schmidt, P. Schwintzer, and U. Send, 2005: Seasonal variation of ocean bottom pressure derived from Gravity Recovery and Climate Experiment (GRACE): Local validation and global patterns. *J. Geophys. Res.*, **110**, C09001, doi:10.1029/2004JC002772.
- Kim, S.-B., T. Lee, and I. Fukumori, 2004: The 1997–1999 abrupt change of the upper ocean temperature in the north central Pacific. *Geophys. Res. Lett.*, **31**, L22304, doi:10.1029/2004GL021142.
- Knudsen, P., 2003: Ocean tides in GRACE monthly-averaged gravity fields. *Space Sci. Rev.*, **108**, 261–270.
- Macdonald, A., and C. Wunsch, 1996: An estimate of global ocean circulation and heat fluxes. *Nature*, **382**, 436–439.
- Marshall, J. C., A. Adcroft, C. Hill, L. Perelman, and C. Heisey, 1997: A finite-volume, incompressible Navier–Stokes model for studies of the ocean on parallel computers. *J. Geophys. Res.*, **102**, 5753–5766.
- Meredith, M. P., and C. W. Hughes, 2004: On the wind-forcing of bottom pressure variability at Amsterdam and Kerguelen Islands, southern Indian Ocean. *J. Geophys. Res.*, **109**, C03012, doi:10.1029/2003JC002060.
- , J. M. Vassie, K. J. Heywood, and R. Spencer, 1996: On the temporal variability of the transport through Drake Passage. *J. Geophys. Res.*, **101**, 22 485–22 494.
- , P. L. Woodworth, C. W. Hughes, and V. Stepanov, 2004: Changes in the ocean transport through Drake Passage during the 1980s and 1990s, forced by changes in the Southern Annular Mode. *Geophys. Res. Lett.*, **31**, L21305, doi:10.1029/2004GL021169.
- Minster, J. F., A. Cazenave, and P. Rogel, 1999: Annual cycle in mean sea level from Topex-Poseidon and ERS-1: Inference on the global hydrological cycle. *Global Planet. Change*, **20**, 57–66.
- Munk, W. H., and E. Palmén, 1951: Note on the dynamics of the Antarctic Circumpolar Current. *Tellus*, **3**, 53–55.
- Olbers, D., D. Borowski, C. Völker, and J.-O. Wölf, 2004: The dynamical balance, transport and circulation of the Antarctic Circumpolar Current. *Antarct. Sci.*, **16**, 439–470, doi:10.1017/S0954102004002251.
- Orsi, A. H., T. Whitworth, and W. D. Nowlin, 1995: On the meridional extent and fronts of the Antarctic circumpolar current. *Deep-Sea Res. I*, **42**, 641–673.
- Parker, R. L., 1975: Theory of ideal bodies for gravity interpretation. *Geophys. J. Roy. Astron. Soc.*, **42**, 315–334.
- Peltier, W. R., 2004: Global glacial isostasy and the surface of the ice-age Earth: The ICE-5G (VM2) model and GRACE. *Annu. Rev. Earth Planet. Sci.*, **32**, 111–149.
- Peterson, R. G., 1988: On the transport of the Antarctic Circumpolar Current through Drake Passage and its relation to wind. *J. Geophys. Res.*, **93**, 13 993–14 004.
- Rintoul, S. R., and S. Sokolov, 2001: Baroclinic transport variability of the Antarctic Circumpolar Current south of Australia (WOCE repeat section SR3). *J. Geophys. Res.*, **106**, 2815–2832.
- , —, and J. Church, 2002: A 6 year record of baroclinic transport variability of the Antarctic Circumpolar Current at 140°E derived from expendable bathythermograph and altimeter measurements. *J. Geophys. Res.*, **107**, C103155, doi:10.1029/2001JC000787.
- Smith, S. D., 1988: Coefficients for sea-surface wind stress, heat flux, and wind profiles as a function of wind speed and temperature. *J. Geophys. Res.*, **93**, 15 467–15 472.
- Song, Y. T., and V. Zlotnicki, 2004: Ocean BP waves predicted in the tropical Pacific. *Geophys. Res. Lett.*, **31**, L05306, doi:10.1029/2003GL018980.
- , and T. Y. Hou, 2006: Parametric vertical coordinate formulation for multiscale, Boussinesq, and non-Boussinesq ocean modeling. *Ocean Modell.*, **11**, 298–332.
- Sprintall, J., 2003: Seasonal to interannual upper-ocean variability in the Drake Passage. *J. Mar. Res.*, **61**, 27–57.
- Swenson, S., and J. Wahr, 2002a: Estimated effects of the vertical structure of atmospheric mass on the time-variable geoid. *J. Geophys. Res.*, **107**, 2194, doi:10.1029/2001JB000515.
- , and —, 2002b: Methods for inferring regional surface-mass anomalies from satellite measurements of time variable gravity. *J. Geophys. Res.*, **107**, 2193, doi:10.1029/2001JB000576.
- , and —, 2006: Post-processing removal of correlated errors in GRACE data. *Geophys. Res. Lett.*, **33**, L08402, doi:10.1029/2005GL025285.
- Tapley, B. D., S. Bettadpur, M. Watkins, and C. Reigber, 2004: The gravity recovery and climate experiment: Mission over-

- view and early results. *Geophys. Res. Lett.*, **31**, L09607, doi:10.1029/2004GL019920.
- Thompson, D. W. J., and J. M. Wallace, 2000: Annular modes in the extratropical circulation. Part I: Month-to-month variability. *J. Climate*, **13**, 1000–1016.
- , and S. Solomon, 2002: Interpretation of recent Southern Hemisphere climate change. *Science*, **296**, 895–898.
- Velicogna, I., and J. Wahr, 2006: Measurements of time-variable gravity show mass loss in Antarctica. *Science*, **311**, 1754–1756.
- Wahr, J., M. Molenaar, and F. Bryan, 1998: Time-variability of the Earth's gravity field: Hydrological and oceanic effects and their possible detection using GRACE. *J. Geophys. Res.*, **103**, 205–230.
- , S. Swenson V. Zlotnicki, and I. Velicogna, 2004: Time-variable gravity from GRACE: First results. *Geophys. Res. Lett.*, **31**, L11501, doi:10.1029/2004GL019779.
- , —, and I. Velicogna, 2006: Accuracy of GRACE mass estimates. *Geophys. Res. Lett.*, **33**, L06401, doi:10.1029/2005GL025305.
- Wang, W., and R. X. Huang, 2004: Wind energy input to the surface waves. *J. Phys. Oceanogr.*, **34**, 1276–1280.
- Wearn, R. B., and D. J. Baker, 1980: Bottom pressure measurements across the Antarctic Circumpolar Current and their relation to wind. *Deep-Sea Res.*, **27A**, 875–888.
- Whitworth, T., III, and R. G. Peterson, 1985: Volume transport of the Antarctic Circumpolar Current from bottom pressure measurements. *J. Phys. Oceanogr.*, **15**, 810–816.
- Woodworth, P. L., J. M. Vassie, C. W. Hughes, and M. P. Meredith, 1996: A test of the ability of TOPEX/POSEIDON to monitor flows through the Drake Passage. *J. Geophys. Res.*, **101**, 11 935–11 947.
- Wu, X., D. F. Argus, M. B. Heflin, E. R. Ivins, and F. H. Webb, 2002: Site distribution and aliasing effects in the inversion for load coefficients and geocenter motion from GPS data. *Geophys. Res. Lett.*, **29**, 2210, doi:10.1029/2002GL016324.
- Wunsch, C., 1998: The work done by the wind on the oceanic general circulation. *J. Phys. Oceanogr.*, **28**, 2332–2340.